31st Annual International Conference of the IEEE EMBS
Minneapolis, Minnesota, USA, September 2-6, 2009

Improved Segmentation of Echocardiographic Images Using Fusion of Images from Different Cardiac Cycles

Junier Caminha Amorim, Maria do Carmo dos Reis, João Luiz Azevedo de Carvalho, Adson Ferreira da Rocha, and Juliana Fernandes Camapum

Abstract — **In this work, an algorithm for the detection of the left ventricular border in two-dimensional long axis echocardiographic images is presented. In its preprocessing stage, images fusion was applied to a sequence of images composed of three cardiac cycles. This method exploits the similarity of corresponding frames from different cycles and produces contrast enhancement in the left ventricular boundary. This result improves the performance of the segmentation stage which is based on watershed transformation. The obtained left ventricle border is quantitatively and qualitatively compared with contours manually segmented by a cardiologist, and with results obtained using seven different techniques from the literature.**

I. Introduction

Several medical image segmentation methods for identification of the left ventricular wall have been proposed in the literature. Image preprocessing has been shown to improve the segmentation in up to 35% [1]. Many algorithms exploit temporal information in the preprocessing stage. For example, de Andrade *et al.* [2] used the pixel average from successive frames, and Choy *et al.* [3] used information from a reference frame border to improve subsequent border extraction.

Some of the left ventricular segmentation works use short axis images [4] [5] while others operate on long axis images [2] [6] [7]. Different approaches were chosen for denoising, such as morphologic filtering [3] [5], the discrete wavelet transform [2], and temporal averaging [4]. Lacerda et al. [6] applied elevation filtering followed by thresholding.

This paper presents a new preprocessing method for left ventricle segmentation in two-dimensional long axis echocardiographic image sequences. The segmentation results are quantitatively and qualitatively compared with contours manually segmented by a cardiologist, and with results obtained using seven different techniques from the literature.

II. Methods

The algorithm was divided into two main stages: preprocessing and segmentation. The sequences of images, composed of three cardiac cycles, are originally stored in DICOM (Digital Imaging and Communications in Medicine) format. In the preprocessing stage, images with a certain degree of similarity, in equivalent positions within the different cardiac cycles, are merged. This process reduces noise and enhances the contrast of the left ventricular wall. This improves the performance of the segmentation stage, which is performed by watershed transformation.

Fig. 1 presents the flowchart of the implemented algorithm, showing the sequence of operations of the two main stages. These are discussed in detail in the next two subsections.

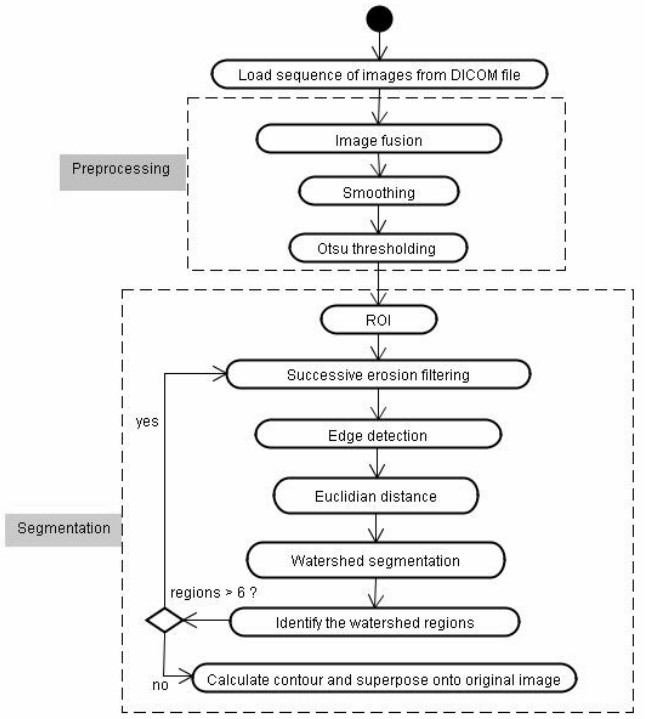

Fig. 1. Flowchart of the left ventricle segmentation algorithm.

A. Image Preprocessing

The heart involuntarily performs an average of about 70 beats per minute, in cycles of contraction (systole) and distention (diastole). These cycles are repeated over time and cause, eventually, more symmetrical states in different time positions. A graphic representation of the cardiac cycles (electrocardiographic signal) is shown in Fig. 2, from which it can be noted that there is significant similarity between the different cardiac cycles. Images obtained at the same cardiac phase, from different cardiac cycles (e.g.,

Manuscript received April 23, 2009.

J. C. Amorim, M. C. dos Reis, J. L. A. Carvalho, J. F. Camapum and A. F. da Rocha are with the Electrical Engineering Department, University of Brasília, Brasília, DF 70910-900, Brazil (e-mail: junieramorim@yahoo.com.br, carminhamcr@yahoo.com.br, joaoluiz@gmail.com, juliana@ene.unb.br, adson@ene.unb.br)

images obtained at the time instant associated with the R wave of the electrocardiogram, i.e., the instant of ventricular contraction), have a high probability of presenting similar cardiac anatomy. Variations in heart volume/position and interbeat interval are not being considered.

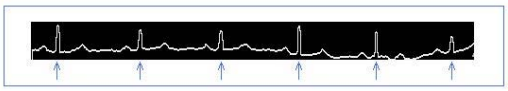

Fig. 2. Cardiac cycles measured by electrocardiography. The R waves, which correspond to ventricular contraction, are indicated.

1) Image Fusion

DICOM files, extracted from echocardiographic equipment, and containing 90 consecutive frames (3 cardiac cycles), were used in this work (30 frames per cardiac cycle). Only normal cardiac cycles were used in this work in order to avoid motion artifacts, i.e., cardiac cycles corresponding to arrhythmias were excluded. A composite image is obtained through the fusion of 9 images, using 3 consecutive images from each of the three cycles (Fig. 3). This produces a set of 28 segmented images, covering a complete cardiac cycle. Grouping is performed for a set of images from approximately the same cardiac phase within each of the three cardiac cycles. An image is produced for each group, in which each pixel position contains the highest gray level observed in the set of 9 images for that particular position. The window length (3 neighboring frames) was heuristically adopted, based on tests made with the method presented in ref. [8]. The use of longer windows causes blurring in the resulting image, due to insufficient temporal resolution.

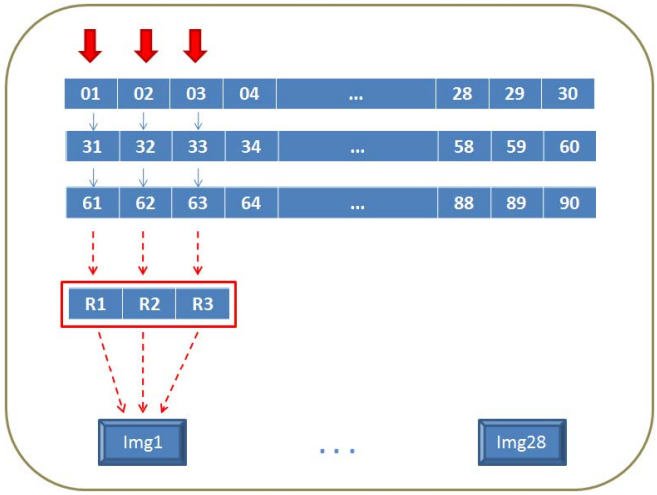

Fig. 3. Diagram showing the images fusion process being applied to a sequence of 90 frames.

The fusion process may be described by the following equations:

$$f_{R1_k}(x,y) = \max\{f_{k-1}(x,y), f_{k-1+N}(x,y), f_{k-1+2N}(x,y)\} \quad (1)$$

$$f_{R2_k}(x,y) = \max\{f_{k}(x,y), f_{k+N}(x,y), f_{k+2N}(x,y)\} \quad (2)$$

$$f_{R3_k}(x,y) = \max\{f_{k+1}(x,y), f_{k+1+N}(x,y), f_{k+1+2N}(x,y)\} \quad (3)$$

$$f_{R_k}(x,y) = \max\{f_{R1_k}(x,y), f_{R2_k}(x,y), f_{R3_k}(x,y)\} \quad (4)$$

where k = 2, 3, …, N−1, is the frame position within the a cardiac cycle (i.e., cardiac phase), N is the number of frames per cycle (i.e., N=30), $f_k(x,y)$ is the k-th image in the image sequence, and $f_{R_k}(x,y)$ is the composite image corresponding to the k-th cardiac phase.

The result of this process is illustrated in Fig. 4, in which a gain in cardiac wall contrast can be noted.

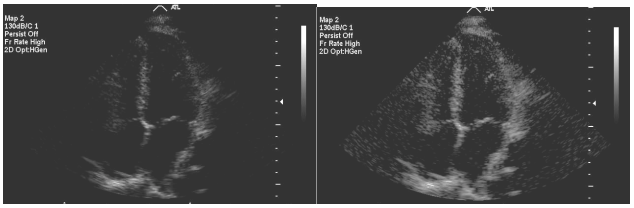

(a) (b)

Fig. 4. Illustration of the proposed image fusion preprocessing method: (a) original image, and (b) associated composite image.

2) Image Smoothing

This step is performed using a Gaussian filter (Fig. 5a).

Before applying the Gaussian filter, the Otsu threshold [9] is calculated to be used later for image binarization. This procedure is done at this point to increase binarization tolerance, by delegating the indirect adjustment of the threshold to the smoothing operator.

3) Thresholding

Otsu thresholding [9], or dynamic thresholding, is applied to the smoothed image using the index calculated in the previous step (Fig. 5b).

B. Watershed Segmentation

1) Region-of-interest identification

The first step in the segmentation stage is the identification of the region-of-interest (ROI) (Fig. 5b). This region encompasses the smallest area of highest probability of covering the left ventricle. This procedure will help the segmentation algorithm because the operations will not be influenced by the part of the image which was eliminated. The DICOM standard ensures the result of this cut operation because these files have the position of the LV in the same region.

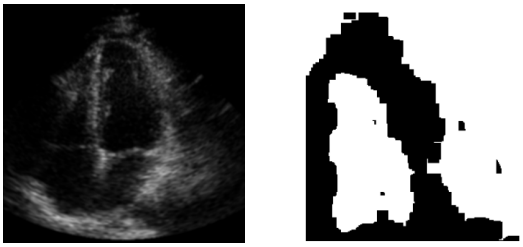

(a) (b)

Fig. 5. (a) image smoothed by Gaussian filter (b) identification of the ROI after Otsu thresholding.

2) Erosion

Within the ROI, morphological operations are performed to reduce image noise. In order to avoid super-segmentation

in the watershed step, successive erosions are applied to reduce image noise and distortion (Fig. 6a). The structuring element is defined by a matrix of size (N_y×0.025, 3), with unit elements (N_y is the number of rows in the image).

One point of concern is the positioning of the mitral valve, which is responsible for connecting the left ventricle to the left atrium. Due to the fusion of images from three different cardiac phases, valve motion causes the region near the mitral valve to appear blurry, potentially causing the junction of the left ventricle with the left atrium. The solution adopted to address this issue was to incorporate a subroutine that counts the number of regions in the image, and thus identify whether or not the two chambers were accidentally connected. When this problem occurs, the image is discarded.

3) Edge Detection

The next segmentation step is to identify the edges of the eroded image (Fig. 6a), using the multiscale gradient (MG) operator [1], which performs successive morphological gradient calculations (ρ) with different structuring elements B_i, through (5) and (6):

$$MG = \frac{1}{n}\sum[\rho(f, B_i) \Theta B_{i-1}] \quad (5)$$

$$P(f, B) = (f \oplus B) - (f \Theta B), \quad (6)$$

where f is the matrix representation of the image. The structuring element B_i is defined by a square matrix of size ($2i$+1), with unit elements. The number of iterations represented by the integer value n may vary, but in practice, it is observed that values higher than 15 cause the total degradation of the image. In this algorithm, the range of n was 1 to 10.

Fig. 6b illustrates the result of the application of multiscale gradient to an eroded image. With this operator, edges with various distances are identified as the structuring elements B_i assume different sizes and can be positioned between one and another. Moreover, the noise content was reduced.

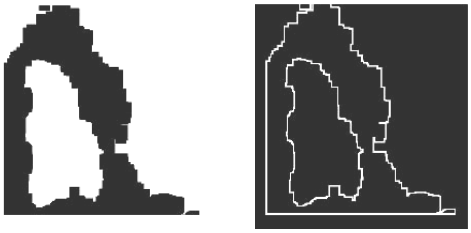

(a) (b)

Fig. 6. (a) Result from successive erosions applied to a binary image, and (b) result from multiscale gradient (MG) applied to the eroded image.

4) Euclidean Distance Transform

In order to calculate the Euclidean distance $d(x,S)$ [10], the region S between the inner and outer border of the MG image must be identified. This was achieved using region filling (Fig. 7a). Then, the distance $d(x,S)$, which is the shortest distance from x (a pixel in S) to the boundary of S, is calculated (Fig. 7b).

(a) (b)

Fig.7. (a) Result from region filling between the inner and outer border of the MG image (Fig. 6b), and (b) result obtained using the Euclidean distance transform.

5) Watershed segmentation

Finally, watershed transformation is applied to the images obtained from the Euclidean distance map. This process segments the image into two regions, background and object. The object represents the contour of the left ventricle (Fig. 8).

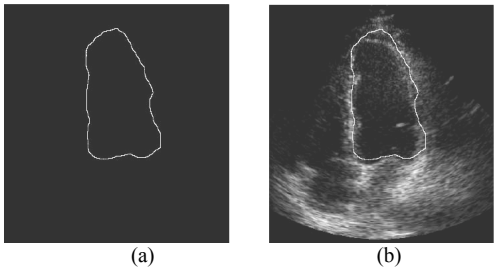

(a) (b)

Fig. 8. (a) left ventricular wall contour, obtained using watershed segmentation to the image in Fig. 6b, and (b) superposition onto original image.

III. Results and Performance Evaluation

A set of 8 long-axis (LA) images from 9 different patients, classified as of high quality by a specialist, were used to evaluate the performance of the proposed algorithm. Low quality images were processed by the automatic algorithm, but could not be properly delineated by the specialist.

The proposed method was compared with six different approaches from the literature, including methods proposed for use with short-axis (SA) images. Two different metrics were used: the error sum (*ES*) [7] and Correlation Index (*CI*) [5]. These metrics estimate the similarity between manually segmented and automatic contours, and were calculated as follows:

$$ES = \frac{\left|M \cap \overline{A}\right| + \left|\overline{M} \cap A\right|}{|M|} \times 100 \quad (7)$$

$$CI = \frac{|M|}{|A|} \text{ if } M \le A \quad CI = \frac{|A|}{|M|} \text{ if } M > A \quad (8)$$

where M and A are the sets of pixels within the manually- and automatically-defined contours, respectively; $|M|$ and $|A|$ are the areas (e.g. the numbers of pixels) from each set. Note that *CI* is an optimistic measure of similarity, since the shape of the contours is not taken into account, but only the areas. However, *ES* compares shapes and represents the non-overlapping areas between $|M|$ and $|A|$.

The quantitative results are shown in Table I, and a qualitative comparison between manual and automatic segmentation is shown in Fig. 9.

TABLE I
COMPARISON BETWEEN PROPOSED APPROACH AND METHODS FROM THE LITERATURE

	# of images	*CI*, μ	*ES*(%), $\mu \pm \sigma$
Proposed method - LA	8	0.917	10.79 ± 2.95
Lilly *et al.* [7] - LA	25	-	11.35 ± 4.22
Sequential radial search [6]-LA	7	-	18.51 ± 5.06
de Andrade *et al.* [2]- LA	20	-	9.62 ± 7.9
Optic Flow [4] - SA	10	-	9.47 ± 2.02
Small Sliding Window [4] -SA	10	-	12.44 ± 2.41
Klinger *et al.* [5] - canine SA	-	0.93	-

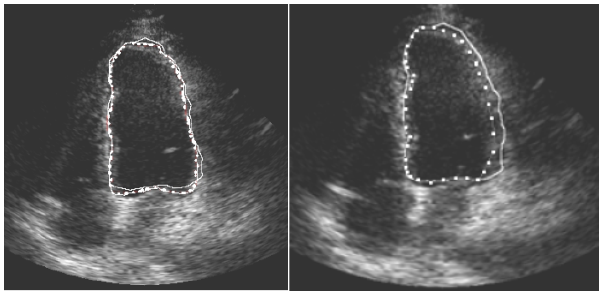

Fig. 9. Superpositon of the left ventricular wall manually-segmented contour (dotted line) onto the automatically-segmented contour, obtained using the proposed method (solid line), in two representative results.

In order to eliminate the statistical difference due to the use of different databases by each author, the proposed method was compared with two different algorithms, using a database composed of 5 long-axis images (Table II).

TABLE II
QUANTITATIVE COMPARISON BETWEEN PROPOSED APPROACH AND METHODS FROM THE LITERATURE, USING THE SAME IMAGE DATABASE (5 LONG-AXIS IMAGES)

	CI, μ	*ES*(%), $\mu \pm \sigma$
Proposed method	0,949	10.79±2.95
Optic Flow [4]	0,95	9.47±2.02
Silva *et al.* [11]	0,897	17.88±3.40

These values confirm the positive impact of the proposed preprocessing algorithm. The results obtained with the proposed method were equivalent or better than those obtained with other methods, for the same database. Furthermore, the optic flow algorithm [4] is computationally-intense (approximately 20 minutes), whereas the proposed method's computational time is approximately 2 minutes, using the same hardware and software. The improvement in segmentation quality due to the preprocessing stage can also be illustrated by the results presented in Fig. 10.

IV. CONCLUSIONS

We presented a semi-automatic solution for efficient segmentation of the left ventricular wall in long-axis echocardiographic images. The algorithm combined image fusion with mathematical morphology for binary images and watershed segmentation. The goal of image fusion is to improve the result of the preprocessing stage, which contributed to increased watershed segmentation accuracy. delineation The quantitative comparison showed that our results are equivalent or more accurate than other methods from the literature. The proposed method may facilitate the diagnosis of cardiac conditions and the process of delineating the ventricular border.

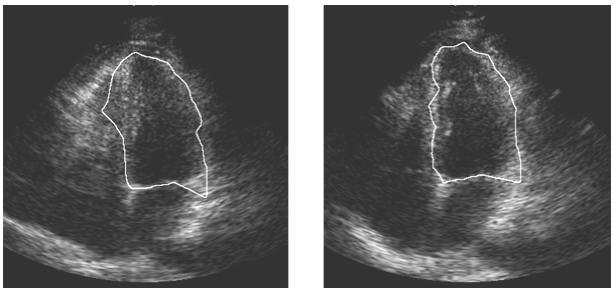

Fig. 10. Results for different preprocessing stage implementations: (a) without image fusion, and (b) with image fusion.

REFERENCES

[1] Gonzalez, R. C., and Woods, R. E., "Digital Image Processing", Addison Wesley Pub. -ISBN: 0201180758, 2º ed, 2001.

[2] de Andrade, M. M., Macchiavello, B., Nascimento, F. A. O., Rocha, A. F. Algoritmo híbrido para segmentação do ventrículo esquerdo em imagens de ecocardiografia bidimensional.Revista Brasileira de Engenharia Biomédica, vol. 22, n. 1, p. 105, 2006.

[3] M. M. Choy and J. S. Jin, "Extracting Endocardial Borders from Sequential Echocardiography Images", IEEE Engineering in Medicine and Biology, p. 116-121, Jan-Feb 1998.

[4] Reis, M. do C. dos; Rocha, A. F. da; Vasconcelos, D. F.; Espinoza, B. M.; Nascimento, F. A. de O.; Salomoni, S.; Camapum, J. F.. "Semi-Automatic Detection of the Left Ventricular Border". 30th Annual International Conference of the IEEE Engineering in Medicine and Biology Society, Vancouver, v. 1, p. 218-221, 2008.

[5] Klinger, J. W. Jr., Vaughan, L.C., Fraker JR., T. D., Andrews, L. T. Segmentation of echocardiographic images using mathematical morphology. IEEE Transactions on Biomedical Engineering, vol. 35,n. 11, p. 925-934, 1988.

[6] Lacerda, S. G., Rocha, A. F. da, Vasconcelos, D. F., Carvalho, J. L. A., Sene Jr., I. G., Camapum, J. F., "Left Ventricle Segmentation in Echocardiography Using a Radial-Search-Based Image Processing Algorithm", 30th Annual International Conference of the IEEE Engineering in Medicine and Biology Society, Vancouver, v. 1, p. 222-224, 2008.

[7] P. Lilly, J. Jenkins, and P. Bourdillon, "Automatic Contour Definition on Left Ventriculograms by Image Evidence and a Multiple Template-Based Model", IEEE Trans. on Medical Imaging, vol. 8, n. 2, pp. 173-185, 1989.

[8] Cheng, Jierong; Foo, Say Wei; Krishnan, Shankar M., "Automatic Detection of Region of Interest and Center Point of Left Ventricle using Watershed Segmentation", IEEE Int. Symposium on Circuits and Systems, vol. 1 n. 2, pp. 149-151, May 2005.

[9] Chai, Yu-hua; Gao, Li-qun; Lu, Shun; Tian, Lei. "Wavelet-based Watershed for Image Segmentation Algorithm", IEEE 6th World Congress on Intelligent Control and Automation, China, 2006.

[10] Fabbri, R.; Costa, L. da F.; Torelli, J. C.; Bruno, O. M. "2D Euclidean distance transform algorithms", ACM Computing Surveys, v. 40, p. 1-44, 2008.

[11] Silva, A. O., Camapum, J. F., Freitas, A. N., Bassani, H. F., Vasconcelos, R. A., Freitas, F. M. O. "Watershed Transform for Automatic Image Segmentation of the Human Pelvic Area", IEEE International Conference on Acoustics, Speech, and Signal Processing, Montreal-ICASSP, v. 5, p. 17-21, 2004.